Journal of Cardiovascular Magnetic Resonance®, 4(2), 211–222 (2002)

METHODS

Fully Refocused Gradient Recalled Echo (FRGRE): Factors Affecting Flow and Motion Sensitivity in Cardiac MRI

Laurie B. Hildebrand and Michael H. Buonocore*

Department of Radiology, University of California Davis Medical Center, Sacramento, California

ABSTRACT

The Fully Refocused Gradient Recalled Echo (FRGRE) magnetic resonance pulse sequence, previously reported as True FISP, was implemented and reported on a GE Signa CV/i 1.5T scanner. The purpose of this research was to optimize the pulse sequence design and scanning parameters to improve image quality for cardiac applications. A 2-D, multi-slice, multi-phase, breathold, segmented k-space, prospectively gated FRGRE sequence was implemented with TE and TR values as short as 0.9 and 3.0 msec, respectively. Pulse sequence design changes were investigated theoretically in terms of moment calculations and by assessing the quality of long- and short-axis cardiac images. The most influential scanning parameter for the improvement of image quality was both a short TR and TE. Placement of the z gradient rephaser immediately before the slice select gradient reduced the accumulated moments and improved image quality. Increasing the slice thickness from 3 to 8–10 mm significantly reduced flow artifact. The number of views per segment was doubled, without decreasing image quality, cutting breathold time in half compared to cardiac scanning with conventional sequences with longer TRs. The optimal flip angle was approximately 60°. The use of a full or fractional echo had no noticeable effect on image quality. Surprisingly, the addition of flow compensation pulses significantly decreased image quality. In summary, optimization of sequence design and scanning parameters significantly reduced flow artifacts seen in FRGRE images.

Key Words: *Cardiac MRI; True FISP; FRGRE; Steady state; Flow artifact*

*Corresponding author. Professor of Radiology and MRI Technical Director, UC Davis Imaging Center, UCDMC, 4701 X Street, Sacramento, CA 95817. E-mail: mhbuonocore@ucdavis.edu

INTRODUCTION

The True Fast Imaging with Steady Precession (True FISP) pulse sequence was first conceived in 1986 by Oppelt et al. (1) and used for cerebrospinal (2) and interventional (3) applications but has not been applied to cardiac imaging until recently as a result of the improvements in gradient hardware. In this research, the implementation of True FISP optimized for reduction of flow and motion artifacts, is referred to as Fully Refocused Gradient Recalled Echo (FRGRE).

The FRGRE sequence is characterized by transverse magnetization that is fully refocused within each TR interval, as compared to other fast scanning methods where the transverse magnetization is refocused in later TR intervals or destroyed by spoiling. The refocusing is carried out in each of the three gradient directions by applying a rephasing gradient of equal and opposite area. The signal is maintained in FRGRE by creating steady state equilibrium between transverse and longitudinal magnetization, using RF pulses with alternating polarity in successive TR intervals.

Imaging the heart using the FRGRE pulse sequence results in images with higher contrast to noise between the blood and myocardial wall and images that are less sensitive to flow resulting in a more uniform blood signal compared to the current industry standards (4–8). The increase in contrast results in easier delineation of cardiac structures, as well as more accurate quantitative measurements within the heart. Since the FRGRE sequence is a fast imaging sequence, the shorter TR values can result in shorter breatholds for the patient and acquisition of more images.

A FRGRE-type pulse sequence optimized for cardiac imaging has been reported in practice on Siemens Medical Systems (Erlangen, Germany) MRI systems (4–8). The purpose of this research was to successfully implement the sequence on a GE Medical Systems (Milwaukee, WI) MRI system, with specific features necessary for cardiac imaging, and optimize the pulse sequence design and scanning parameters to maximize image quality and reduce flow and motion artifacts.

METHODS

A 2D, segmented, multi-slice, multi-phase, breatheld, FRGRE sequence was designed with EPIC (Environment For Pulse Programming in C) Software Version 8.2.5 from GE Medical Systems (Milwaukee, WI) and implemented on a GE Signa CV/i 1.5T system (Milwaukee, WI) with prospective cardiac gating (9,10). Figure 1 shows the pulse sequence diagram. The sequence maintained steady state by alternating the

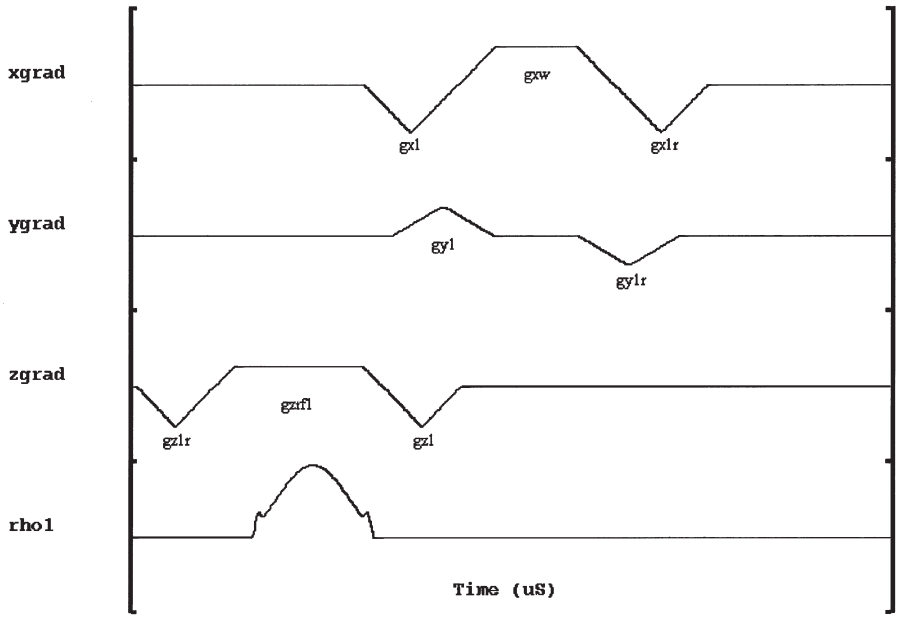

Figure 1. This pulse sequence timing diagram depicts one TR interval in the FRGRE sequence with TE = 1.2 and TR = 3.2 msec. The gradients are balanced in area over each TR interval for *x*, *y*, and *z*. The rho1 line represents the 0.496 msec RF pulse.

amplitude of a 0.496 msec RF pulse, designed with the Shinnar-Le Roux algorithm, by 180° while maintaining a receiver phase shift of zero. The RF pulse continuously alternated polarity throughout data acquisition while waiting for the appropriate cardiac trigger. Gradient pulses were created with the shortest possible plateau time. The following typical imaging parameters were used: 3.2 msec TR, 1.2 msec TE, 28 cm FOV, 256 × 128 matrix, 6 mm slice thickness, 125 kHz receiver bandwidth, 60° flip angle, 81.6 kg patient weight, and a centered echo in a traditional orthogonal plane. To achieve high speed imaging, system specifications must include a receiver bandwidth of 125 kHz or greater, a maximum gradient slew rate of at least 150 mT/m/sec, and maximum gradient amplitude of at least 40 mT/m. Within each TR interval, after all gradient waveforms are completed, a wait time, in which there is no gradient or RF pulse activity, is needed for system processor board updates. If the wait time is too short the sequence halts. On the CV/i system, this wait time varies between 140 and 400 μsec, depending on the acquisition parameters and must be determined empirically. This wait time varies among manufacturers and system models.

In order to reduce the flow artifacts, a flow compensated sequence was also created. Figure 2 shows the pulse sequence diagram. Flow compensation waveforms were added in the readout and slice directions. Calculations by Bernstein et al. (11) were used to derive the flow compensated gradient waveforms. The resulting TR and TE were 4.8 and 1.8 msec, respectively. The resulting gradient waveforms were not slew rate limited, however, with the typical scanning parameters, the fastest possible slew rates, relative to the derived slew rates, reduced TR by only 76 μsec. This improvement was not large enough to justify further refinements in calculating the gradient waveforms. Typical scan parameters used were 256 × 128 matrix, 5 mm slice thickness, 32 cm FOV, 125 kHz receiver bandwidth, and 60° flip angle.

It was verified that the FRGRE sequence signal levels were in agreement with previously reported results using True FISP. The signal levels of FRGRE shown in Fig. 3 were calculated using the following equation from Zur et al. (12).

$$S = \frac{e^{-TE/T2}(1 - E1)\sin\alpha}{1 - (E1 - E2)\cos\alpha - (E1)(E2)} \quad (1)$$

where, α = flip angle, $E1 = \exp(-TR/T1)$, $E2 = \exp(-TR/T2)$, M_0 is taken to be 1.0. The signal intensity for the above equation is very high. If T1 = T2 and TR $\ll$ T1 and T2 then the signal will approach 0.5, one-half of the thermal equilibrium signal. The contrast varies according to T2/T1 when assuming TR $\ll$ T1 and T2, and using a large flip angle. As shown in Fig. 3, the

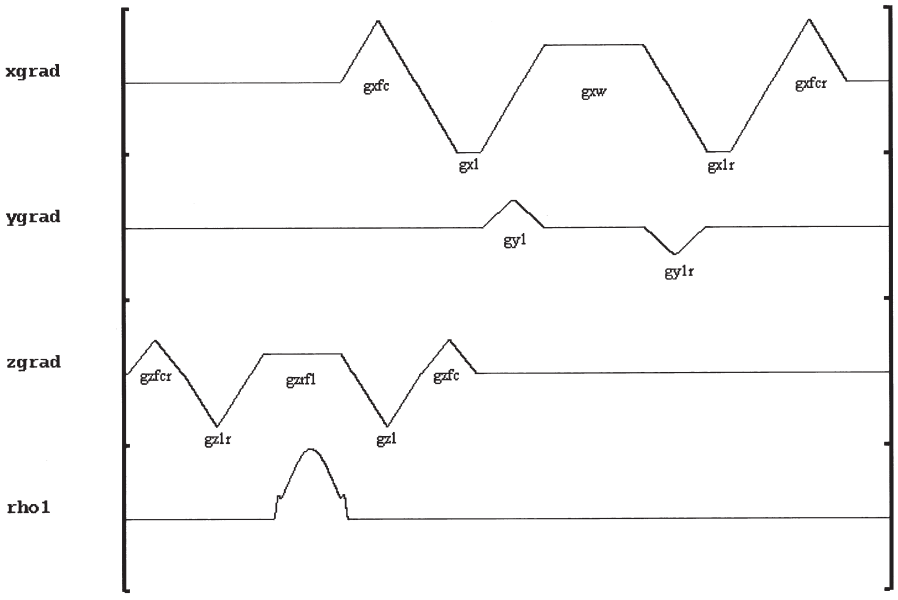

Figure 2. This pulse sequence timing diagram depicts the flow compensated FRGRE sequence. The extra gradients gxfc, gxfcr, gzfc, and gzfcr are added for flow compensation resulting in a TR = 4.8 and TE = 1.8 msec.

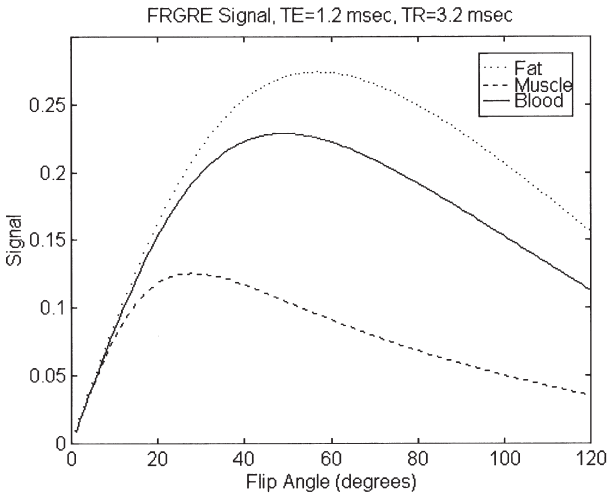

Figure 3. In the FRGRE sequence the signal for blood peaks at 49°, fat peaks at 57°, and muscle peaks at 28°. The maximum signal difference for blood and muscle is at 64°. Note for these calculations TR = 3.2 msec, TE = 1.2 msec, T1(blood) = 1200 msec, T2(blood) = 250 msec, T1(fat) = 284 msec, T2(fat) = 84 msec, T1(muscle) = 759 msec, and T2(muscle) = 47 msec.

FRGRE steady state signal of blood peaks at 49°, and the largest signal difference between muscle and blood occurs at a flip angle of 64°. This theoretical prediction served as an estimate of the flip angle needed to achieve maximum contrast between blood and myocardium in cardiac applications.

Scans were performed to compare signal levels of FRGRE with those of Fast GRE and Spoiled Gradient Recalled Echo (SPGR). The signal levels from the FRGRE sequence were consistently higher than the signal levels for all other sequences. The theoretical signal level of blood served as a rough approximation to the signal level of blood in the image because disruption of steady state magnetization, due to flow effects on magnetization amplitude and phase, were not modeled.

The phase, ϕ, that accumulated in a group of spins in the presence of a time varying magnetic field gradient, $\mathbf{G}(t)$, was written as:

$$\phi(\mathbf{r},t) = \gamma\int_0^t \mathbf{G}(t)\cdot\mathbf{r}(t)\mathrm{d}t,$$

$$\mathbf{r}(t) = \mathbf{r}(0) + \mathbf{r}'(0)t + \mathbf{r}''(0)\frac{t^2}{2} + \cdots \quad (2)$$

$\mathbf{r}(t)$ was the motion vector with the first term representing the position, the second term representing the motion due to constant velocity, and the third term representing the motion due to constant acceleration at $t = 0$. The remaining terms in $\mathbf{r}(t)$ were computed by the Taylor expansion and represented the higher order terms. Therefore, phase accumulated at the initial position of a group of moving spins represented the zeroth moment and was written below:

$$M_0 = \phi_{0,r} = \gamma\mathbf{r}(0)\cdot\int_0^t \mathbf{G}(t')\mathrm{d}t' \quad (3)$$

The phase accumulated due to a constant velocity, or first moment, was written below:

$$M_1 = \phi_{1,r} = \gamma\mathbf{r}'(0)\cdot\int_0^t t'\mathbf{G}(t')\mathrm{d}t' \quad (4)$$

As reported by Zur et al. (13), when the gradients were balanced in area, the zeroth moment nulling ($M_0 = 0$) was achieved over the TR interval. This was the case for FRGRE in the x, y, and z axes. Moment calculations for the FRGRE sequence were created using the EPIC.

For FRGRE parameter and sequence design optimization, scans were performed on five healthy subjects (one male and four female), who ranged in age from 24 to 55 years and gave informed consent. Scans were performed to compare image quality using different scan parameters and sequence designs. Each comparison was done in at least two subjects. For each comparison, representative images were taken from one of the subjects for use in the article.

RESULTS

Pulse Sequence Design

Z Gradient Rephaser

The placement of the z gradient rephasing lobe, *gz1r*, within the TR interval had a significant effect on image quality. Figure 4 shows the *gz1r* lobe placed directly before the slice select gradient. This placement eliminated the zeroth moment and reduced the first moment at the center of the slice select gradient to 0.23° per (cm/sec). The zeroth and first moments of the gradient waveform over the entire TR interval were also eliminated. The even symmetry of the waveform, which gives rise to zero M_1 over the entire TR interval, is easily seen in this figure. Figure 5 shows *gz1r* separated from the slice select gradient. With this placement, the zeroth moment is nulled at the center of the slice select gradient

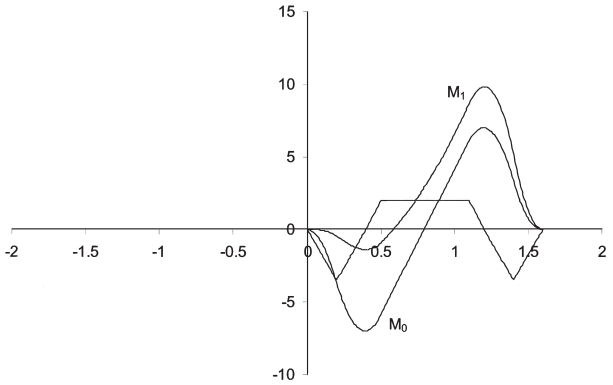

Figure 4. This figure shows a portion of the z gradient axis when the rephasing lobe is placed immediately before the slice select gradient. Note the zeroth moment, M_0, is nulled at the center of the slice select gradient. The first moment, M_1, is approximately 0.23° per (cm/sec) at the center. Both M_0 and M_1 are nulled over the TR interval.

demonstrating that the transverse magnetization refocuses at the center of the slice select gradient. In Fig. 5, the first moment over the entire TR interval is nonzero making the signal intensity more sensitive to flow.

A difference in the image quality was noted between the two placements of the *gz1r* gradient lobe, Fig. 6. During periods of high flow during systole, the image with a separated *gz1r* demonstrated a severe phase-encode artifact (Fig. 6B). This is explained by the large M_1 across the TR interval, which represents increased sensitivity to changes in velocity. From Fig. 5 the lack of symmetry, due to the separation between *gz1r* and the slice select gradient, and the nonzero M_1 are clear. For comparison, the symmetry of the gradient waveform that occurs when *gz1r* immediately precedes the slice selection gradient gives rise to zero M_0 and M_1 over the entire TR interval and results in a reduction in phase-encode artifact demonstrated in Fig. 6A.

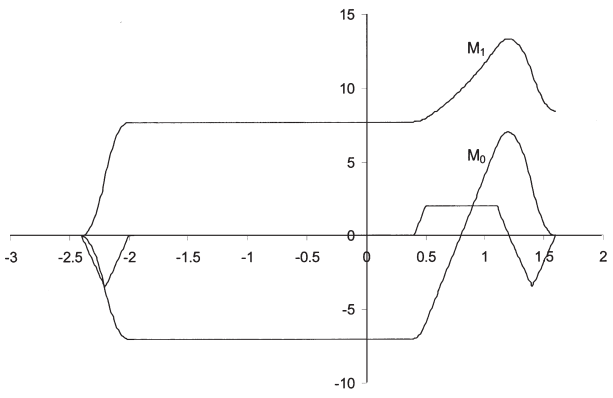

Figure 5. This figure depicts the z gradient axis when the rephasing lobe is separated from the slice select gradient. Note the zeroth moment, M_0, is nulled at the center of the slice select gradient and over the TR period. The first moment, M_1, accumulates phase over the TR interval.

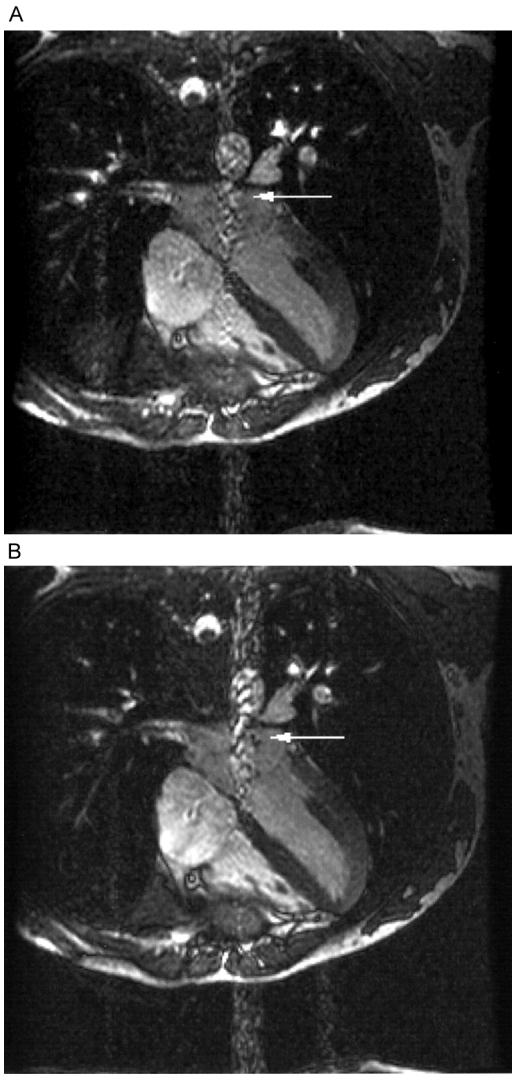

Figure 6. Note the decreased artifact from the aorta when the *gz1r* gradient is placed immediately before the slice select gradient (A) vs. when the gradients are separated (B). The artifact extends across the image in the phase direction and exhibits the typical FRGRE banding pattern. The images are acquired at the same cardiac phase.

Full vs. Fractional Echoes

The zeroth and first moments were calculated for the case of a full and fractional echo. A full echo occurs when the echo is centered in the middle of the readout gradient. With a full echo, the zeroth and first moments are zero over the TR interval, as shown in Fig. 7. At the echo, the zeroth moment is zero and the first moment is approximately 0.2° per (cm/sec).

With the 66% fractional echo, the echo occurs left of middle in the readout gradient. The zeroth moment is zero at the echo, and over the entire TR interval, Fig. 8. The first moment is approximately 0.05° per (cm/sec) at the echo, and approximately −0.31° per (cm/sec) over the entire TR interval.

For cardiac imaging, the fractional echo provides TE as short as 0.9 msec, which is approximately 0.3 msec shorter than when using a full echo. In imaging studies, only small differences existed in the image quality between the case of a full and fractional echo. The full echo resulted in slightly clearer boundaries between the blood and myocardium. There was no significant difference in signal intensity using full vs. fractional echo.

Flow Compensation

For an oblique scan prescription, flow compensation resulted in a TE of 2.2 msec and a TR of 5.7 msec, as indicated in Fig. 9. A test was performed to verify that blurring seen in the flow compensated FRGRE was due to the large TE and TR. Extra time was added to the TE and TR of a nonflow compensated FRGRE sequence to match the TE and TR values of the flow compensated sequence. At the same TE and TR values, the image quality was poor with both flow compensation and no flow compensation sequences. Flow artifacts were equally severe in the images.

Scanning Parameters

TE and TR

Imaging time proved critical to image quality. In Fig. 10, the TR interval was increased from 3.3 to 5.0 msec while all other imaging parameters including TE remained constant. There was a significant decrease in image quality with the longer TR. To test the effect of TE, the TR was held at 4 msec and the TE was varied

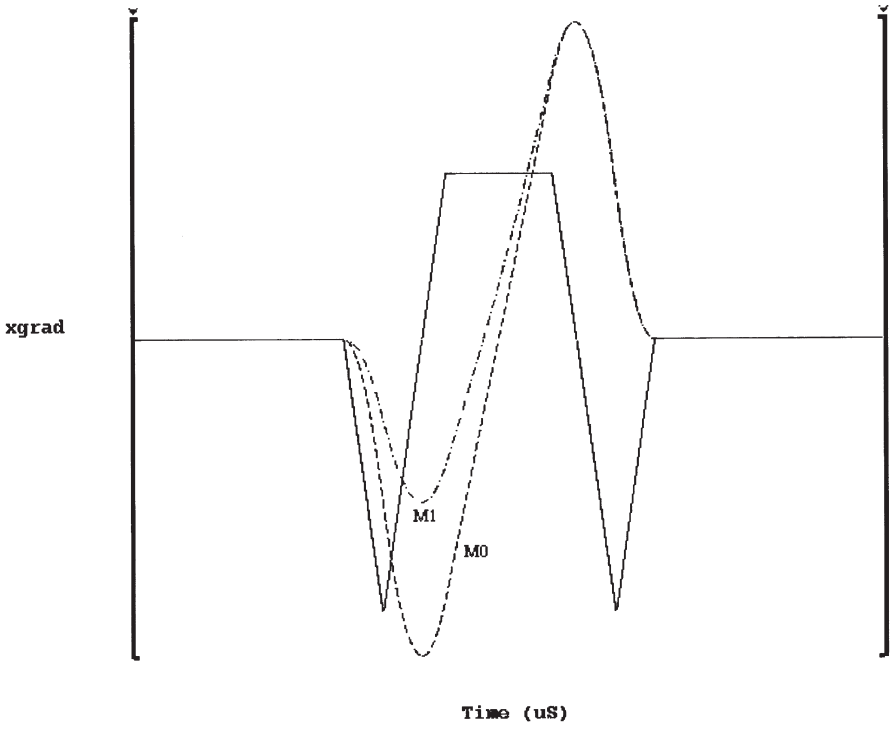

Figure 7. This figure depicts the *x* gradient axis with a full echo. Note the zeroth moment, M_0, is nulled at the echo. The first moment, M_1, is approximately 0.2° per (cm/sec) at the echo. Both M_0 and M_1 are nulled over the entire TR interval.

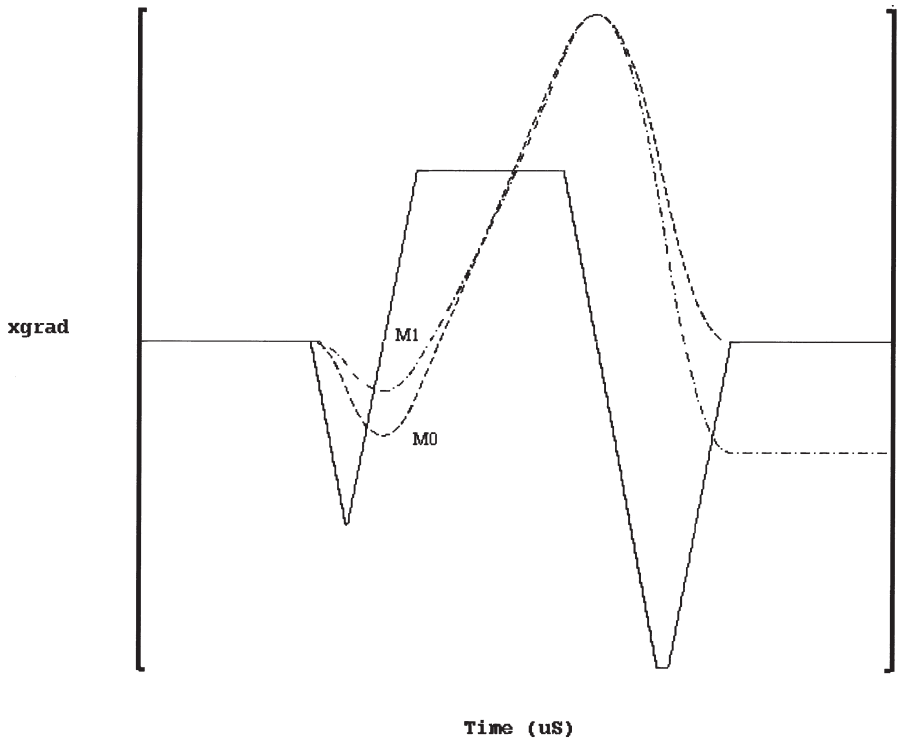

Figure 8. This figure depicts the *x* gradient axis with a fractional echo. Note at the echo, occurring to the left of the center, the zeroth moment is nulled and the first moment is approximately 0.05° per (cm/sec). Phase accumulates from the first moment over the TR interval.

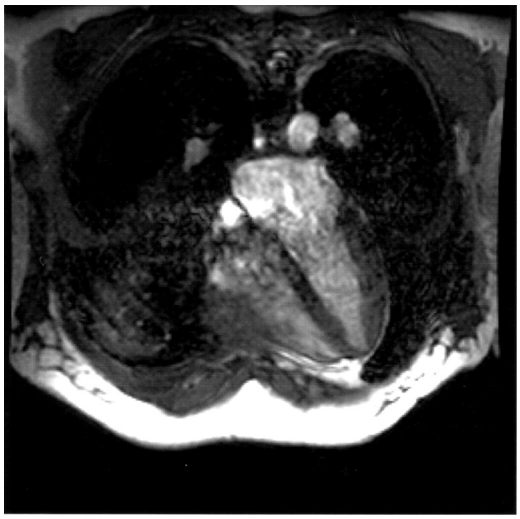

Figure 9. Flow compensation is used here. The large artifact is due to the longer TE of 2.2 and TR of 5.7 msec. The slice thickness is 6 mm.

from 1.3 to 1.6 msec. As shown in Fig. 11, the image obtained with the shorter TE had significantly less artifact.

Slice Thickness

Slice thickness also influenced the image quality. Figure 12A shows a 10 mm slice in which essentially no artifact was created by aortic flow during mid-late systole (frame 21 of a total of 47 acquired over 90% of the cardiac cycle). Figure 12B shows a 6 mm slice, in which a significant artifact was created during this period. The differences in image artifact between a 6 and 10 mm slice were minimal during late systole and diastole.

A combination of both a thicker slice and shorter TR resulted in improved image quality. The images in Fig. 13 demonstrated these improvements. The long-axis end systolic image (frame 34 of a total of 47 representing 90% of the cardiac cycle) in Fig. 13A,

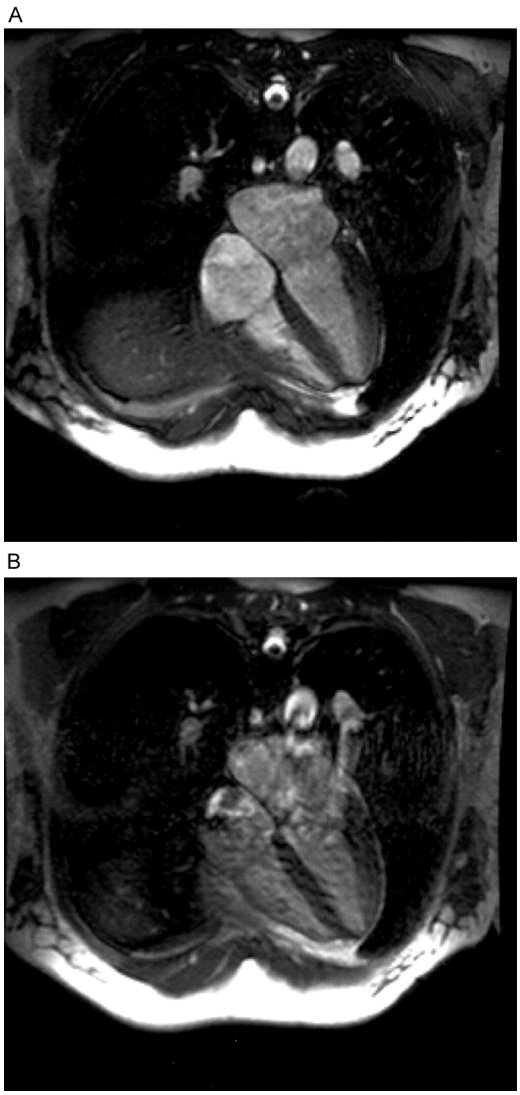

Figure 10. These images show the effect of TR on image quality. At the 3.3 msec TR, the artifact is greatly reduced in the image (A). At the 5.0 msec TR, large artifacts are present throughout the entire image (B). The only difference in the acquisition of the images is the TR time. The images are acquired at the same cardiac phase with the same TE interval.

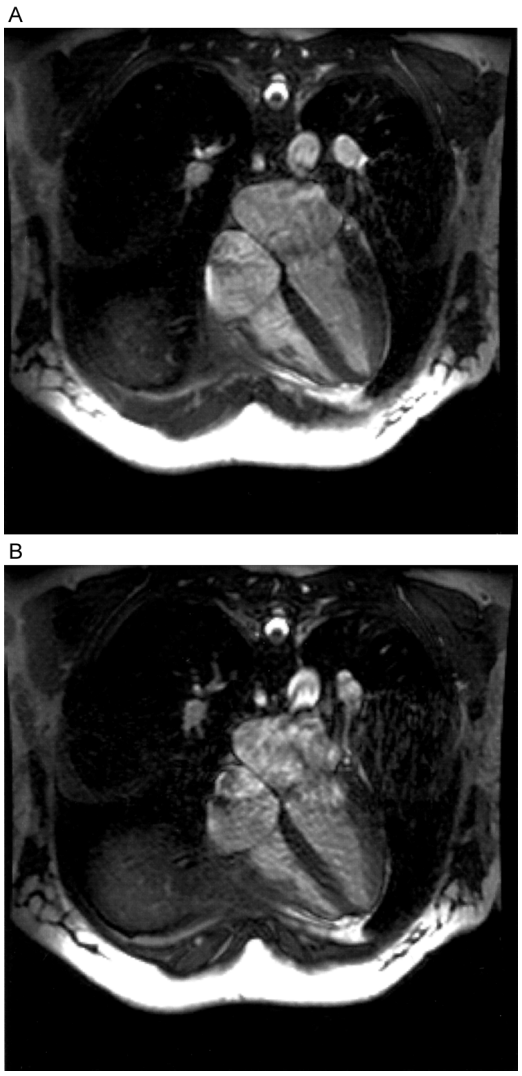

Figure 11. These images show the effect of TE on image quality. The image obtained with TE = 1.3 msec (A) has significantly less artifact than the image obtained with TE = 1.6 msec (B). Both images have the same TR of 4 msec. All other imaging parameters are identical.

had a 3.2 msec TR and 6 mm slice thickness. Figure 13B has a 3.7 msec TR and a 3 mm slice thickness. All other imaging parameters, in particular the end-systolic phase of the cardiac cycle, were identical. The primary difference in image artifact was the absence of the flow artifact from the aorta during ejection in Fig. 13A.

Flip Angle

The signal dependence on flip angle was also tested. The difference in signal between flip angles of 50 and 60° was measured for one subject. No difference in signal was noted in the long-axis view at TE = 1.2 msec and TR = 3.3 msec. In the short-axis view at TE = 0.9 msec and TR = 3.6 msec the myocardial signal was approximately equal for flip angles of 50° and 60°. However,

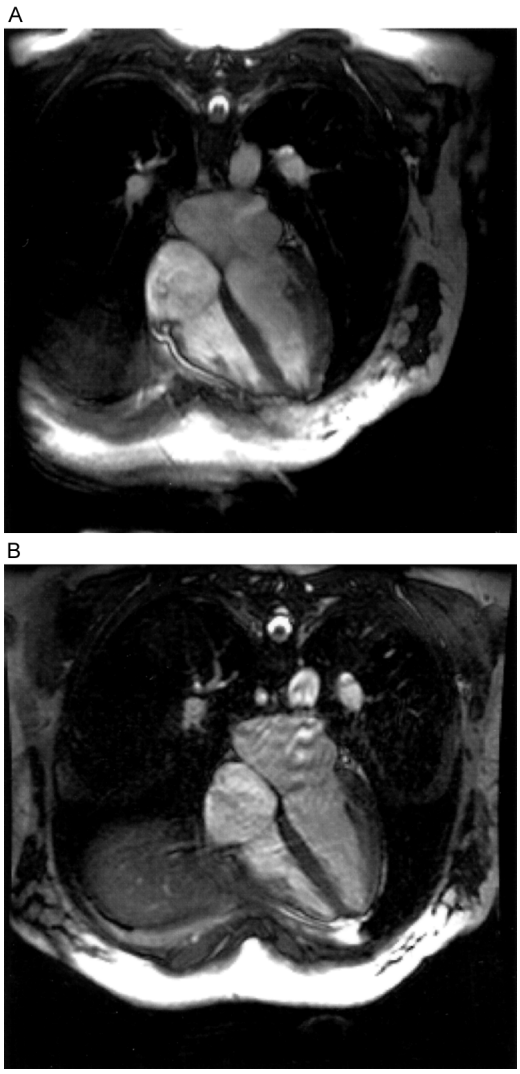

Figure 12. These images at mid-late systole show the effect of slice thickness on image quality. During aortic ejection, the artifact is considerably less in the 10 mm (A) slice as compared to the 6 mm slice (B). Also note these images were obtained on slightly different scan planes because the scan plane must be re-prescribed when changing from a 6 to 10 mm slice.

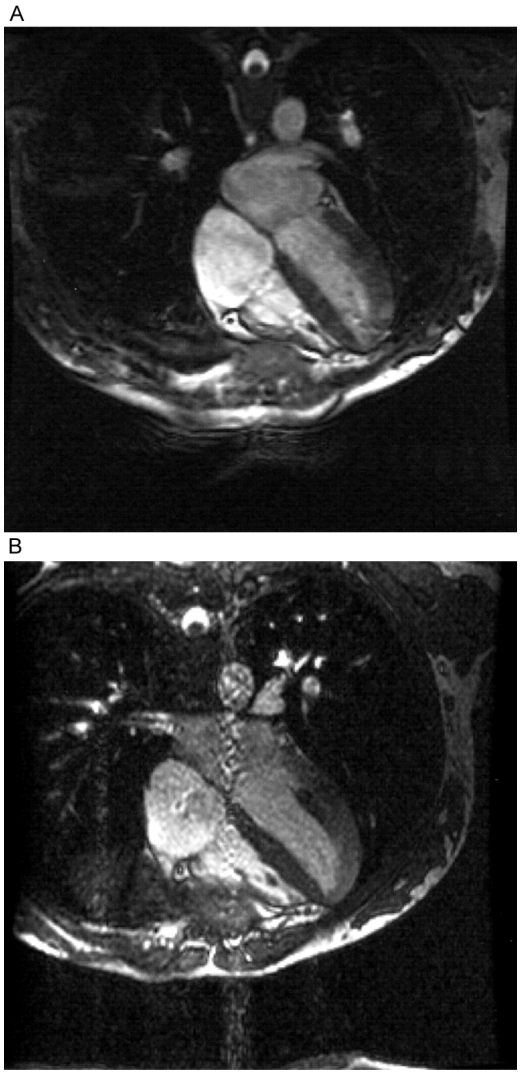

Figure 13. These images depict the combined effect of TR and slice thickness on image quality. In (A), the TR is 3.2 msec and slice thickness is 6 mm. In (B), the TR is 3.7 msec and slice thickness is 3 mm. The image quality of (A) is significantly better than that of (B) because of a shorter TR and a thicker slice. The images are acquired during the same cardiac phase at different scan planes. Compared to Fig. 12B, (A) has a shorter TR and acquired at a different cardiac phase, i.e., end systole vs. mid-late systole.

with respect to the blood signal in the left and right ventricles, the signal-to-noise ratio (SNR) was much higher with a 60° flip angle, as compared to the 50° flip angle. The blood image intensity using flip angles of 50 and 60° averaged between 323 and 413, respectively. Standard deviation of the noise was six, based upon the variations of background image intensity following a Rician distribution. Therefore, the SNRs using flip angles of 50° and 60° were 53.8 and 68.8, respectively. The improvement in SNR using the larger flip angle was 28%.

Views per Segment (VPS)

The VPS refers to the number of phase encoding lines acquired in each defined cardiac phase. Adjusting the

VPS affected image quality, the number of cardiac phases that can be defined across the RR interval, and the breathold time. Increasing VPS resulted in more blurring due to cardiac motion, fewer defined cardiac phases, but shorter breathold times. These trade-offs are listed in Table 1, assuming a heart rate of 70 beats per minute and no view sharing. Using the FRGRE sequence, no differences in image quality were discernable with a VPS of 8 vs. 14, but image quality was slightly degraded with a VPS of 20. Due to shorter TR, FRGRE with a VPS of 20, requiring an 8 sec breathold, provided comparable image quality to Fast SPGR with a VPS of 8, which required a 16 sec breathold.

DISCUSSION

This article documents the significant flow artifacts that can occur in FRGRE imaging and the selection of scan parameters to minimize them. An analytical description of the flow artifact specific to FRGRE is not currently available, but it is believed that the flow artifacts reported in this article are due to the usual causes described as variable inflow enhancement, phase dispersion signal loss, and beat to beat variation of magnetization phase.

Pulse Sequence Design

Several pulse sequence design parameters influenced image quality in FRGRE, such as the placement of the *gz1r* rephasing gradient. Even though separating the *z* gradient rephasing lobe from the slice-select gradient reduced the TR slightly, it drastically increased the moments generated during slice selection and across the TR interval, and thereby decreased image quality. Therefore, the *z*-gradient rephasing lobe was always placed at the beginning of the TR directly before the slice select gradient.

Imaging with a full or fractional echo was comparable in FRGRE. The slightly clearer blood/myocardium boundaries achieved with the full echo is most likely the result of acquiring higher spatial frequencies in the readout direction, which are not acquired with the fractional echo. Nevertheless, the fractional echo provided shorter TE times and a smaller first moment at the echo, theoretically reducing flow artifact. However, the fractional echo provided a greater accumulated first moment over the entire TR interval, theoretically increasing flow artifact. On the basis of the scans conducted in this research, there was no clear advantage in image quality for either method.

Table 1

Views per Segment	Cardiac Phases	Breathold (sec)
8	47	16
14	25	10
20	17	8

Flow compensation (i.e., first moment nulling) failed to provide an improvement in image intensity and uniformity of flowing blood. Both flow compensated, and nonflow compensated, FRGRE were performed using $TR = 4.8$ and $TE = 1.8$ msec. Flow-related artifacts were severe in the noncompensated FRGRE, as expected, based upon the relatively long TR and TE. Flow compensation was performed in both frequency encode and slice select directions, and artifacts were equally severe to those seen in the noncompensated sequence. Flow artifacts are caused by variability in the amplitude and phase of equilibrium transverse magnetization in successive TR intervals. The failure of artifacts to be removed by flow compensation suggests that variable amplitude due to flow of blood into the slice (i.e., inflow enhancement), rather than variable phase due to velocity (i.e., velocity-dependent phase dispersion), is the main cause of flow-related artifacts. Blood inflow primarily disrupts the longitudinal component of equilibrium magnetization from one TR interval to the next, which leads to variability of transverse magnetization and, hence, signals each phase encode step. Had variable phase (of the transverse component of magnetization) due to velocity been the main cause of the flow artifacts in the nonflow compensated sequence, the artifacts would have been reduced by first moment nulling. Variable phase due to higher orders of motion (e.g., acceleration) contribute in both sequences.

Scanning Parameters

A short TR and TE were both essential for good image quality in FRGRE. When trying to determine if it was better to have a shorter TR or shorter TE, no conclusion was drawn. Images with a longer TR (Fig. 10B) and a longer TE (Fig. 11B) are equally bad. Shorter imaging times increased image quality most likely due to the reduction of all moments. The TR intervals less than approximately 3.5 msec were recommended when FRGRE cardiac imaging or large image artifacts occurred.

Increasing the slice thickness decreased the spatial resolution resulting in signal averaging and a smoother appearance. Increasing the slice thickness also decreased image artifact. With a thicker slice, a smaller proportion of spins not in steady state contributed to the signal. The difference in image quality due to slice thickness was most notable during systole. The 6 mm slice in Fig. 12 was reconstructed from data taken in mid to late systole. The ventricle is contracted, and flow in the descending aorta is relatively high. Relative to the 6 mm slice thickness, the 10 mm slice thickness reduces the substantial inflow effects. The 6 mm slice shown in Fig. 13 was reconstructed from data acquired in end systole, just prior to opening of the mitral and tricuspid valves. The period of highest flow in the descending aorta had passed already, so this image with a 6 mm slice thickness has considerably less artifact than the image with the 6 mm slice thickness in Fig. 12. Slower forward and swirling blood flow within the descending aorta gives rise to inflow artifacts only on the thinner slice images. The recommended slice thickness to minimize artifact is 6–10 mm.

Theoretically, the maximum difference in signal between the blood and myocardium occurred at 64°, and the peak blood signal occurred and 49° for TR = 3.2 and TE = 1.2 msec. In cardiac scans, the blood signal levels at 60° were approximately equal in the short-axis view and higher in the long-axis view than those at 50°. Therefore, a 60° flip angle was chosen as the optimal angle. The difference between the two views was probably due to differences in the proportion of blood flowing into the slice in the two slice orientations.

Because of shorter TR of the FRGRE sequence, VPS can provide combinations of breathold times and temporal resolution that are not available with conventional CINE GRE sequences. For example, using FRGRE with a VPS of 20, the time spent acquiring lines for each cardiac phase is approximately 60 msec (3 msec × 20 = 60 msec), and the breathold time can be reduced to 8 sec. By comparison, using Fast SPGR with a VPS of 8, the time spent acquiring lines for each cardiac phase is 72 msec (9 msec × 8 = 72 msec), and the breathold time is 20 sec. Thus, compared to Fast SPGR, FRGRE provides comparable temporal resolution with much shorter breathold times.

Consistency of Results

Although each parameter comparison was not performed on all subjects, image differences were clearly seen and were consistent in all subjects used for each comparison. The differences were not subtle and are believed to represent fundamental image quality issues. The *gz1r* gradient placements and the use of full vs. fractional echo were tested in two subjects. Comparison of nonflow comp sequences with flow comp sequences, using padding of the TR and TE in the nonflow comp sequence to match the sequence parameters, was also tested in two subjects. Long and short TE and TR comparisons were made in all subjects. Image quality degradation with thinner slices was observed in subjects during sequence development, and a direct comparison using three different slice thicknesses was made in one subject. The dependence of image quality on VPS was observed in subjects during sequence development, and a direct comparison using three different VPS values was made in one subject. Signal levels in blood and myocardium using one flip angle (60°) was measured in all subjects, and representative data from one subject was reported in the article. Dependence of FRGRE image intensity on flip angle was evaluated in one subject, using both cardiac and knee scans.

CONCLUSION

The FRGRE pulse sequence for CINE cardiac imaging was successfully implemented on the GE Signa CV/i scanner. Changes in pulse sequence design and scanning parameters impacted image quality for cardiac scans. Shorter TR and TE, thicker slices, and *z* gradient rephaser lobe placement immediately before the slice-select gradient minimized the flow artifact. The use of fractional echoes was possible and shortened the TE time. Flow compensation was not beneficial because of the significant increase in TE and TR. The FRGRE sequence offered a significant improvement in image quality and scan time compared to other currently used cardiac sequences. The driving factor that influenced image quality was a short TE and TR.

ACKNOWLEDGEMENTS

LBH would like to thank the UCDMC Department of Radiology, UCD Biomedical Engineering Graduate Group, and GE Medical Systems for financial support.

REFERENCES

1. Oppelt, A.; Graumann, R.; Barfub, H.; Fischer, H.; Hartl, W.; Schajor, W. FISP—A New Fast MRI Sequence. Electromedica **1986**, *54*, 15–18.

2. Haacke, M.E.; Wielopolski, P.A.; Tkach, J.A.; Modic, M.T. Steady-State Free Precession Imaging in the Presence of Motion: Application for Improved Visualization of the Cerebrospinal Fluid. Radiology **1990**, *175*, 545–552.
3. Duerk, J.L.; Lewin, J.S.; Wendt, M.; Peterslige, C. Remember True FISP? A High SNR, Near 1-Second Imaging Method for T2-Like Contrast in Interventional MRI at 0.2 T. J. Magn. Reson. Imaging **1998**, *8*, 203–208.
4. Golfarb, J. W.; Li, W.; Griswold, M. A.; Prasad, P. V.; Edelman, R. R. Contrast Enhanced Breath-Hold 3D Coronary Magnetic Resonance Angiography, Proceedings of the ISMRM Fifth Scientific Meeting and Exhibition, Vancouver, B.C., Canada, 1997; 441.
5. Bundy, J.; Simonetti, O.; Laub, G.; Finn, J.P. Segmented TrueFISP Cine Imaging of the Heart, Proceedings of the ISMRM Seventh Scientific Meeting and Exhibition, Philadelphia, PA, 1999; 1282.
6. Jerosch-Herold, M.; Huang, H.; Wilke, N. Magnetization Prepared True FISP Myocardial Perfusion Imaging, Proceedings of the ISMRM Seventh Scientific Meeting and Exhibition, Philadelphia, PA, 1999; 1882.
7. Bundy, J. M.; Laub, G.; Kim, R.; Finn, J. P.; Simonetti, O.P. Real-Time Data Acquisition for LV Function, Proceedings of the ISMRM Seventh Scientific Meeting and Exhibition, Philadelphia, PA, 1999; 386.
8. Fang, W.; Pereles, F.S.; Bundy, J.; Kim, R.; Wu, E.; Simonetti, O. Evaluation Left Ventricular Function Using Real-Time TrueFISP: A Comparison with Conventional MR Techniques. Abstr. J. Cardiovasc. Magn. Reson. **1999**, *1* (4), 310–311.
9. Buonocore, M. H.; Hildebrand, L. Fully Refocused Gradient Recalled Echo (FRGRE) Pulse Sequence for Cardiac Applications in Magnetic Resonance Imaging. University of California Case No. 2000-506-1. Patent Pending.
10. Hildebrand, L. Implementation and Analysis of the FRGRE Pulse Sequence for Cardiac Applications in Magnetic Resonance Imaging. Masters Thesis, University of California at Davis, 2000.
11. Bernstein, M.A.; Shimakawa, A.; Pelc, N.J. Minimizing TE in Moment-Nulled or Flow-Encoded Two- and Three-Dimensional Gradient-Echo Imaging. J. Magn. Reson. Imaging **1992**, *2* (5), 583–588.
12. Zur, Y.; Stokar, S.; Bendel, P. An Analysis of Fast Imaging Sequences with Steady-State Transverse Magnetization Refocusing. Magn. Reson. Med. **1988**, *6*, 175–193.
13. Zur, Y.; Wood, M.L.; Neuringer, L.J. Motion-Insensitive, Steady-State Free Precession Imaging. Magn. Reson. Med. **1990**, *16*, 444–459.

Received September 1, 2000
Accepted September 21, 2001